University of Bath

Alternative formats
If you require this document in an alternative format, please contact:
openaccess@bath.ac.uk

Use of Vapochromic Crystals to Measure the Concentration of a Gaseous Throughflow at the Solid-Fluid Interface

C. M. Sangan[*] · O.J. Pountney · J.A. Scobie · B. Cochrane · C. Stubbs[†] · P.R. Raithby

Abstract

This paper demonstrates the potential of vapochromic crystals as a sensing medium for measurements of local species concentration. Vapochromic crystals exhibit a reversible colour change based on the adsorption and desorption of water. As the water content of the crystals changes so too does the wavelength of light that they reflect (*i.e.* they change colour). In the situation where humid air mixes with a dry gas, the resulting specific humidity of the mixture can be related to the concentration level of the dry gas through a simple mass balance. As far as the authors are aware, this is the first time that vapochromic crystals have been used in this context.

A number of the factors that affect the colour change of the crystal are investigated through simple flat plate experiments in a small wind tunnel. In all experiments, the hue and intensity of the vapochromic crystal was measured as a function of local dry gas concentration; in this case CO_2. Green intensity levels exhibited the broadest activity over the widest range of CO_2 levels, and was therefore used to quantify concentration.

The crystals demonstrated a pronounced hysteresis, where the adsorption and desorption of water into the crystal structure was shown to occur at different concentration levels. The transition band was also shown to be highly temperature dependent when tested over a range of 22-44°C. The vapochromic crystals were assessed for repeatability and found to sense the local CO_2 concentration to ±1.5% CO_2 over a range of green intensity values from 90 to 170. A practical example is presented to show how vapochromic crystals could be applied to the mixing of fluid streams in gas turbine film cooling.

Nomenclature

c	concentration
T	temperature
u	streamwise component of velocity
U_0	free-stream velocity
y	crosswise distance from test plate
θ	relative lighting angle
Θ	relative camera angle
δ	boundary layer thickness
η	adiabatic effectiveness

Subscripts

∞	free-stream
c	coolant
ad	surface

1   Introduction

Experimental fluid dynamicists seeking to make measurements at a solid-fluid interface are chiefly concerned with measurement of the following parameters: pressure, temperature, heat flux and shear stress. Measurement of these parameters can be readily made at discrete surface locations: wall tappings are connected to piezoelectric pressure sensors for measurement of static pressures; thermocouples are attached to the surface, either through adhesion, peening or welding, for measurement of temperatures; thin film gauges are bonded to the surface to determine convective heat fluxes in experiments with heat transfer; and wall shear stress can be determined using floating element sensors.

For experiments with multiple fluid streams that undergo mixing the measurement of an additional parameter at the surface also becomes useful: species concentration. By seeding one of the pre-mixed flows with a tracer gas, such as CO_2, it is possible to discern through measurement of tracer gas concentrations at the surface how the seeded flow mixes out as it is interacts with the unseeded gas stream(s). This can be done at discrete locations using wall tappings that are plumbed into infrared gas analysers (for example, see Sangan *et al.* [1]).

While measurements at discrete locations often provide sufficient information for gaining an appreciable understanding of an experimental condition, there are cases where it is necessary to obtain a spatially resolute array (or 'surface map') of measurements over a test surface. For such cases,

---

[*] C.M. Sangan · O.J. Pountney · J.A. Scobie · B. Cochrane (email symbol)
Department of Mechanical Engineering,
University of Bath, Bath BA2 7AY, UK
e-mail: c.m.sangan@bath.ac.uk
[†] C. Stubbs · P.R. Raithby
Department of Chemistry,
University of Bath, Bath BA2 7AY, UK

experimental fluid dynamicists use films, oils and paints (referred to from hereon in as '*surface coating techniques*') that are applied to the test surface in thin layers. The following surface coating techniques are those used most widely:

- Pressure sensitive paint (PSP) – for measurement of air pressure on a surface.
- Thermochromic liquid crystals (TLC) – for measurement of surface temperatures (and inference of heat fluxes in transient heat transfer experiments).
- Oil-film interferometry (OFI) - for measurement of wall shear stresses.

Surface maps of trace gas concentration can be inferred from pressure measurements made using PSP. The PSP is used to measure oxygen partial pressures with and without the trace gas present; the associated change in partial pressure between the two cases can be used to compute the concentration of the tracer gas (see Han and Rallabandi [2]). Given the time constraints associated with many research programmes, having to carry out *two* tests to produce a single data map is undesirable and so the use of PSP as a means of generating surface concentration maps has tended to be fairly limited.

This paper presents an alternative technique to PSP for measurement of surface gas concentrations in a *single* fluid dynamic experiment: vapochromic crystals. Vapochromic crystals exhibit a reversible colour change based on the adsorption and desorption of water. A number of the factors that affect this colour change are investigated in this paper through simple flat plate experiments. As far as the authors are aware, this is the first time that vapochromic crystals have been used in this context.

Section 2 reviews TLC, PSP and OFI surface coating techniques so as to identify factors that typically affect the reactivity of surface coatings. Section 3 provides an overview of the chemistry governing the behavior of the vapochromic crystals. Section 4 presents the experimental setup used to investigate how the reactivity of the vapochromic crystals is influenced by the factors identified in Section 2; the results of these experiments are discussed in Section 5. Section 6 briefly considers how vapochromic crystals could be used in fluid dynamic experiments through a practical example. It is hoped that the work presented in this paper demonstrates the suitability of vapochromics for use in fluid dynamic experiments and will encourage others to use them in future.

2 A review of surface coating techniques employed in experimental fluid dynamics

TLC, PSP and OFI surface coating techniques are those most widely used by experimental fluid dynamicists. The reaction of these surface coatings when exposed to a stimulus typically involves a change in intensity or colour that is filmed over the course of an experiment. The subsequent image is then post-processed to convert the intensity/colour change of the coating into meaningful data. Factors that affect the reaction of the coating must be accounted for through calibration under experimentally representative conditions if accurate measurements are to be obtained from the images. The review of the surface coating techniques presented in this section identifies those factors known to have the most significant influence on the reactivity of TLC, PSP and OFI; the impact of a number of these factors on the reactivity of vapochromic crystals is subsequently investigated.

2.1 Thermochromic Liquid Crystals (TLC)

TLC are cholesteric crystals that undergo a phase change from solid to liquid when heated. During this phase change the molecular structure of the TLC is modified: the director of adjacent planes rotate relative to one another as a function of temperature. The relative angle of the directors between adjacent planes determines the wavelength of light reflected by the TLC and so the colour change of the crystals is directly related to their temperature (see Fig. 1). Interested readers are referred to Kasagi *et al.* [3] and Ireland and Jones [4] for a detailed description of the theory underpinning the behavior of TLC.
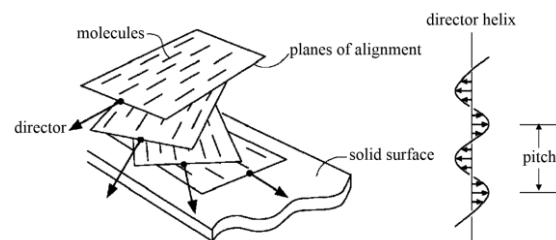
Figure 1: Representation of TLC structure (from Ireland and Jones (2000))

TLC are widely used by experimental fluid dynamicists to measure surface temperature histories during transient heat transfer experiments (for example, see Pountney *et al.* [5]). A fine layer of TLC (typically <50μm) is applied in micro-encapsulated form, most effectively through spraying (Baughn [6]) onto a surface pre-coated with black paint (used to enhance the brightness of the TLC). The light reflected by the TLC layer is largely dependent upon the temperature of the surface. The colourplay of the TLC (change from red to green to blue) occurs over a 1 to 20°C bandwidth with a starting temperature of between -30 and 115°C; TLC with a bandwidth of <5°C are referred to as narrowband crystals and those with a bandwidth of >5°C are referred to as wideband crystals. It is a technique typically used to determine surface maps of adiabatic wall temperature and heat transfer coefficient in transient heat transfer experiments

There are a number of factors that affect the colour change with temperature of TLC. Calibration

must account for *all* of these factors if results are to be obtained with reasonable levels of uncertainty. It is unknown which of these factors (if any) affect vapochromic crystal colour change, but the following list provides a useful starting point for investigation:

- Film thickness – Abdullah *et al.* [7] found that the green intensity calibration curve for their narrowband TLC shifted by 0.4°C when increasing film thickness from 10μm to 50μm; they also observed an 18% increase in peak green intensity.
- Ageing – Kakade *et al.* [8] repeatedly heated narrowband TLC through their colour change limit. The authors showed that cyclic heating produced significant shifts in the calibration curves of their TLC (0.2°C for five heating cycles of a 15μm thick layer of narrowband TLC); it was also observed that thicker layers were more resistant to ageing.
- Hysteresis – Anderson and Baughn [9] observed that heating and cooling produced different hue-temperature curves for a given TLC, noting that researchers must calibrate for the direction of use in their experiments to obtain accurate results.
- Light source – Anderson and Baughn [10] investigated the effect of full-spectrum, fluorescent and tungsten based illumination sources on the hue-temperature curves of their TLC. The authors discovered that UV light rapidly damaged the crystals; they also showed that it was important to perform a white balance at the start of testing to ensure consistency in colour reproduction.
- Lighting and viewing angles – Camci *et al.* [11] and Farina *et al.* [12] showed that off-normal illumination significantly affected colourplay of their TLC, particularly for wideband crystals (0.6°C for a change in lighting angle of 20°C). Kakade *et al.* [8] investigated illumination angle and found similar results; they also discovered that changing the viewing angle of the camera had a similar effect on their calibration curves to changing the illumination angle.

2.2 Pressure-Sensitive Paint (PSP)

McKeon and Engler [13] provide a comprehensive description on the theory of PSP and its use in experimental fluid dynamics. PSPs comprise dye molecules ('*luminophores*') contained in a binder that permeates oxygen. Photons are absorbed by the luminophores – this causes them to transition to an excited state. The luminophores return to their unexcited state through dissipation of energy, which occurs through emission of photons (at a wavelength greater than the illumination source) or through collision with surrounding oxygen molecules – see Fig. 2. The higher the partial pressure of oxygen at the surface of the PSP, the greater the concentration of oxygen molecules within the permeable binder – this increases the number of oxygen-luminophore collisions, thereby reducing energy discharge through photon emission (*i.e.* a higher concentration of oxygen will lower the intensity of the luminescence of the PSP). The intensity of the luminescence of PSP can be calibrated against air pressure (and thus oxygen partial pressure) to provide a useful technique for measuring surface pressures and, indirectly, trace gas concentration levels (see Han and Rallabandi [2]). The technique has generally been used to study external aerodynamics and film cooling of gas turbine blades.
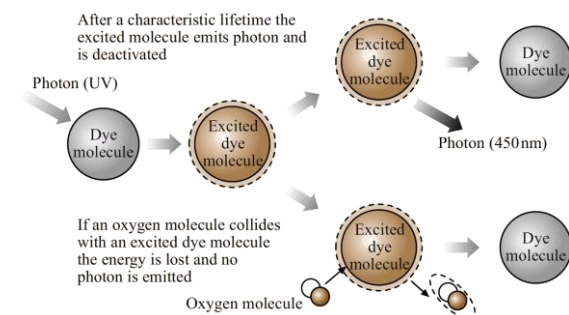
**Figure 2. Schematic of oxygen quenching (from McKeon and Engler (2007)).**

Liu and Sullivan [14] identified 15 factors that affect the uncertainty in pressure measured using PSP. These can be broadly split in four categories:

- *Performance of the camera and light source* – photodetector noise and variation in the spectral output of the illuminator can introduce uncertainties in the measured intensity.
- *Photodegredation and contamination of the surface* – repeated exposure to a high energy illumination source can result in a temporal reduction in the luminescent intensity of the PSP. Contamination of the surface with particulates has a similar effect (these surface particulates absorb the incoming excitation light and outgoing luminescent light to reduce the overall intensity of emission).
- *Model motion* – deformation of the model between 'wind-on' and 'wind-off' conditions (or indeed the relative deformation between different flow conditions) affects the homogeneity of the paint thickness, dye concentration and illumination level over the surface. These factors all affect the calibration of the PSP – their variability over the deformed surface will increase the uncertainty in the measured pressures.
- *Temperature* – of all the factors considered by the authors, temperature was found to have the greatest impact on measurement uncertainty. McKeon and Engler [13] suggest that for some PSPs the error in measured

pressure can be as high as 5% per °C deviation from the baseline calibration temperature – careful temperature control is therefore essential in experiments using PSP.

2.3 Oil-Film Interferometry (OFI)

Klewicki *et al.* [15] present a useful review of OFI for measurement of surface shear stress in wall-bounded flows. A thin film of oil applied to the surface of interest is illuminated by a monochromatic light source to produce fringe patterns (the result of constructive and destructive interference between the light partially reflected off the surface and the light that propagates through the film). The shear force exerted on the oil layer by a fluid flowing over the surface will cause temporal thinning, the rate of which can be used to evaluate the wall shear stress (Tanner and Blows [16]). The spatial variation of the oil film thickness can be determined from the spacing between consecutive dark fringe bands. The rate of change of fringe spacing ('*fringe velocity*') is measured during the course of an experiment using a CCD camera, and is post-processed to determine the wall shear stress – various methods for doing this are described in Naughton and Sheplak [17]. A typical OFI experimental setup is shown in Fig. 3.
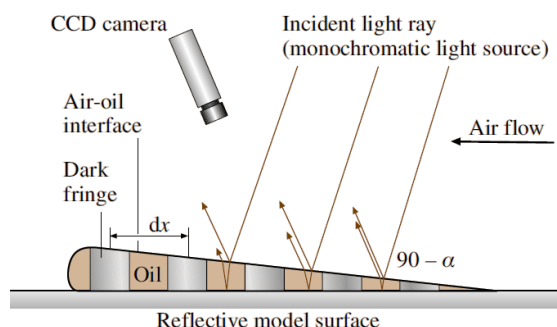
Figure 3. Typical OFI experimental setup (from Klewicki *et al.* [15])

An array of factors affecting the accuracy of OFI are put forward by Klewicki *et al.* [15], not all of which are relevant to this study. Those most pertinent to vapochromic crystals are surface contamination (analogous to thermal ageing and photodegredation of TLC and PSP respectively) and temperature. Naughton and Sheplak [17] identified uncertainty in oil viscosity (required to process the wall shear stress) as the greatest source of error in OFI measurements. It is well-established that viscosity is a function of temperature, and so, as for the PSP measurement technique, OFI relies upon careful control of surface temperature during an experiment if accurate measurements are to be obtained.

3 Vapochromism

Among vapochromic materials phosphorescent square-planar platinum(II) complexes are an active and developing area of research [18] because of the numerous systems that show solid-state vapochromic responses to small molecules analytes 19-21]. The vapochromic behavior in these materials is related to the Pt…Pt interactions in the solid-state, and minor changes in local environment through exposure to chemical vapor perturb these interactions that induce significant changes in their absorption and emission properties [18, 19, 22, 23]. Square-planar cyclometallated Pt(II) pincer complexes are of particular interest because of their luminescence and because of the ease with which they can be manipulated [24].

In this study the vapochromic crystals are comprised of a platinum(II) complex, supported by a tridentate pincer ligand and a cyanide group, and have the formula Pt(N^C^N)(CN), where (N^C^N) = methyl 3,5-di(2-pyridyl)benzoate [25]. The hydrated form, Pt(N^C^N)(CN).H_2O, is red and the anhydrous form is yellow. At the molecular level the complex is essentially flat, and these flat molecules pack in stacks in the solid state so that the d_{z^2} orbitals on adjacent platinum(II), which lie perpendicular to the plane of the molecules, overlap and are partly responsible for the colour of the solid material. In the hydrated form of the complex the water molecules hydrogen-bond adjacent platinum complexes together so that the Pt…Pt stacking distance between molecules is short enough for there to be a significant Pt…Pt interaction, giving the red colour. In the anhydrous complex there is no hydrogen bonding between adjacent complexes and the Pt…Pt distance is longer, with no significant Pt…Pt orbital overlap, causing the colour of the material to change to yellow. The water in the material can easily be lost or absorbed through sub-nanometer channels that run through the crystalline structure. The loss of water from the hydrated (red) form (**Form I**) is readily achieved by blowing dry N_2 or a N_2/CO_2 mixture over a thin film of the vapochromic crystalline material, as shown in Fig. 4, to give the yellow anhydrous form (**Form II**). Removal of the dry N_2 gas stream results in an immediate rehydration of the crystalline material to **Form I** as atmospheric water is absorbed through the sub-nanometer channels in the crystals. The color change is reversible by repeated exposure to dry gas and atmospheric air as shown in Fig. 5. The reversibility occurs on over a period of 100-500 milliseconds depending on the exact characteristics of the thin film [25, 26].
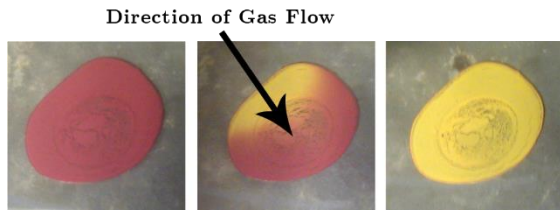
Figure 4: Transition of crystal from Form-I to Form-II (adapted from Bryant [26])
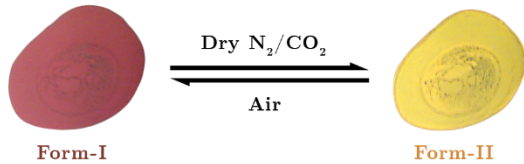

Figure 5: Transition reaction between Form-1 and Form-II

4   Calibration facility and method

In all calibrations, the hue and intensity of the vapochromic crystal was measured as a function of local CO_2 concentration. The crystal was applied to two test plates, both of which could be mounted within a small wind tunnel. The design of the test facility and test plates are described below.

4.1   Calibration apparatus

A schematic of the purpose-built wind tunnel facility is shown in Fig. 6, along with a close-up of the test section (inset). A centrifugal blower was used to create mainstream velocities up to 20 m/s through the test section (Cho *et al.* [27]), which had a cross-section of 20 mm x 100 mm and a length of 120 mm. The chemical composition of the mainstream flow was controlled by injecting CO_2 upstream of the test section; the concentration of CO_2 was varied between 0.003% and 100%. Complete mixing of the CO_2 with ambient air was ensured by installing a Kenics Static Flow Mixer downstream of the CO_2 injection points. After passing through the test section the flow was then exhausted through the laboratory wall.

The test section was modular, allowing for two test plates configurations to be installed: one designed for fluid mechanics experiments and one for elevated temperature conditions. Both test plates housed glass slides on which the vapochromic crystals were applied. The slides were recessed so as to be flush-mounted with the wetted inner surface of the wind tunnel. The inner surface of the back plates were sprayed with black paint (Hallcrest SPBB) to provide contrast to the colour change of the crystals; o-rings were used to seal the plates against the frame of the test section.
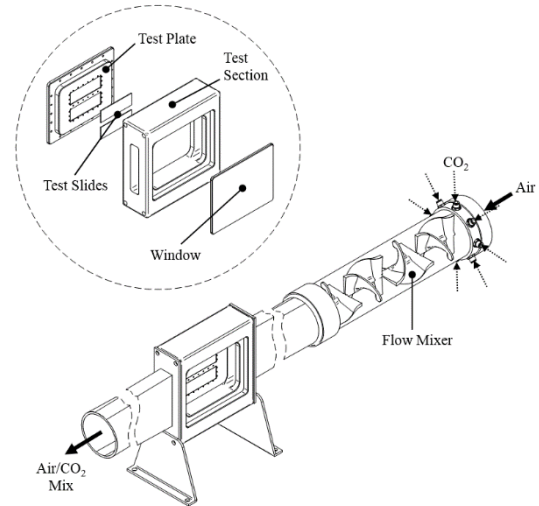

Figure 6: Schematic of the through-flow calibration tunnel. Exploded view of test section shown inset.

The first test plate was made from aluminium and designed for fluid mechanics measurements (shown in Fig. 7a). It featured a series of thirty 1.7 mm diameter holes drilled perpendicular to the mainstream gas path. Stainless steel hypodermic tubing was inserted into each of the holes forming ports for extracting gas samples or making pressure measurements. The holes were equally-spaced around the perimeter of both glass slides.
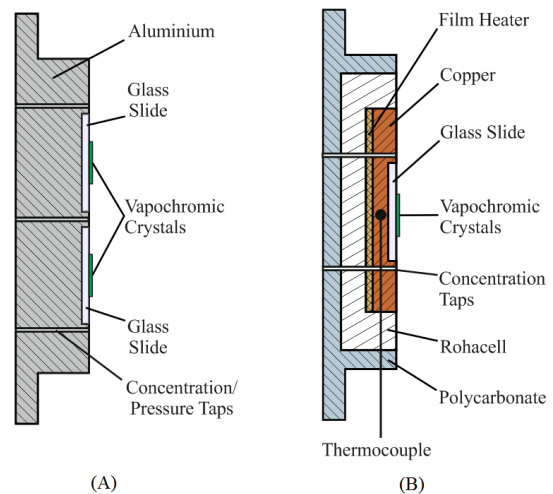

Figure 7: Cross-section views of the assembled test plates: a) fluid mechanics plate, b) elevated temperature plate.

A second test plate was used to conduct experiments at elevated temperatures (shown in Fig. 7b). This geometrically-similar plate was manufactured from polycarbonate and used to house a 65 x 65 x 5 mm copper block, mounted in Rohacell insulating foam (thermal conductivity, *k*, of 0.04 $Wm^{-1}K^{-1}$). The glass slide on which the vapochromic crystals were deposited was recessed into the copper block. A 50 x 50 mm Omega Kapton-insulated foil heater was adhered to the back face of the copper block with thermal paste. The heater was used to

5

control the temperature of the copper block which, owing to its high thermal conductivity, created an isothermal heating of the vapochromic crystals. The temperature of the block was monitored using an embedded K-type thermocouple.

A viewing window made from optical-grade polycarbonate was installed directly opposite the test-plates.

4.2 Testing methodology

The calibration experiments were conducted in a dark room. An off-axis LED light was used to illuminate the test section; a CCD camera (Sony HDR-XR200) was used to capture the colour change of the vapochromic crystals. The camera and light were positioned at relative angles Θ and θ to the perpendicular axis of the test plate, respectively, as illustrated in Fig. 8. The camera and light were fixed at $\Theta = 0^o$ and $\theta = 30^o$ in all calibrations beside those in §5.4. The lighting condition and camera settings (white balance and aperture) were fixed between experiments.
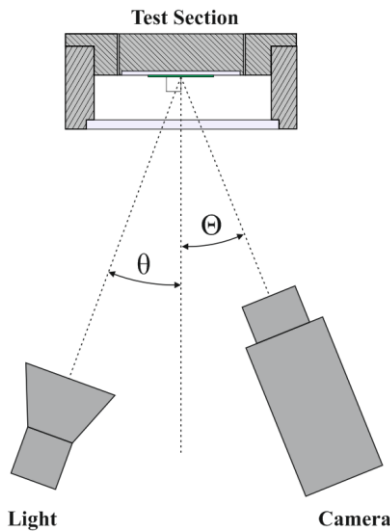

Figure 8: Relative lighting and camera angles for calibration

Concentration measurements were made using a Signal Group 9000MGA gas analyser with a 0-100% CO_2 range. Samples were provided to the unit using a pump, drawing samples from any of the connected hypodermic ports described in §4.1. The gas analyser was calibrated using an alpha-grade span gas of nominal 80% CO_2 and 20% N_2, and a research-grade zero gas of 100% N_2.

Experiments were conducted at a range of mainstream flow concentrations. For all conditions the standard deviation in measured CO_2 concentration between sampling taps was within the experimental uncertainty of the gas analyser: >0.5% of the full scale range. The data presented in §5 was therefore taken from only one centrally located sampling port, directly between the glass slides.

Measurements of total and static pressure were taken to ensure a turbulent boundary layer profile existed in the test section. A pitot-tube was installed through one of the sampling ports in the test plate; the pitot tube could be traversed across the test section using a micrometer. A static pressure tap on the wall of the test section was used in combination to assess the velocity distribution across the tunnel using Bernoulli's principle. The differential pressure between the two ports was measured using a pressure transducer with uncertainty of +/- 0.75 Pa.

The velocity distribution in the test section is shown in Fig. 9. The local velocity was normalized to that of the free-stream and is plotted as a function of the non-dimensional distance from the wall. The boundary layer thickness was 5.5 mm, defined when $u(y) = 0.99U_0$. The experimental data is shown to conform to the theoretical $1/7^{th}$ power law for a turbulent boundary layer. The uncertainty in measured values of u/U_0 is +/- 0.025.
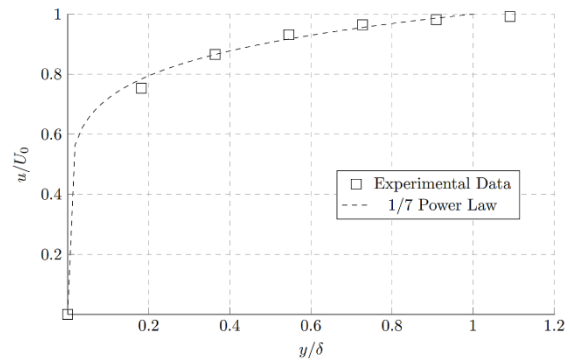
Figure 9: Velocity distribution in the test section

All experimental data was acquired through a National Instruments Compact DAQ, which provided the raw voltage signals to a custom-built LabVIEW software interface. The LabView data logger triggered a digital time counter that was positioned within the field of view of the camera. This ensured synchronicity between data acquisition and image capture.

4.3 Image processing

The image processing was conducted using MATLAB R2015b, employing the Image Processing Toolbox. Each calibration image contained a 50 x 50 pixel square. A 5 x 5 median filter (*medfilt2* in MATLAB) was used on each of the RGB image components to reduce the effect of experimental uncertainty on the result. The filter, as described by Baughn *et al.* [28], directly replaces the RGB values in each pixel with the median of the values contained in all adjacent blocks. The mean value within the filtered 50 x 50 pixel image was then converted to hue and intensity using the MATLAB function, *rgb2hsv*. The use of a median filter on the RGB data before calculating the hue is now an established process when image processing

5   Demonstration of vapochromic materials as a sensing medium

The crystals were observed to be a uniform red colour under ambient conditions (*i.e.* an unseeded through-flow). On increasing the concentration of CO_2 in the mainstream flow, the crystals changed from red (**form-I**) to yellow (**form-II**) through a range of shades of orange. The colour change process was found to be reversible when the CO_2 concentration was subsequently lowered, *i.e.* the crystals returned from **form-II** to **form-I**. The following sections present the basic colour change calibration before examining the crystal performance with respect to hysteresis, viewing angle, aging and response at elevated temperature.

5.1   Basic color change calibration

Two basic calibrations were conducted: **form-I** to **form-II** and **form-II** to **form-I**. Fig. 10 shows the variation of hue and intensity with CO_2 concentration in the through-flow (images of the crystal are shown, inset) for **form-I** to **form-II**. The mass flow-rate of air in the wind tunnel and the injection rate of CO_2 were controlled to incrementally increase the gaseous CO_2 level in steps of 2-4% up to 100%; for all cases the CO_2 level was measured by infra-red gas analysis – as discussed in §4.2.

It can be seen that the vapochromic crystals are insensitive to CO_2 concentration levels below ~85%. A rise in green and red intensity levels was seen after this point, with a change in blue intensity, and ultimately hue, not seen until CO_2 concentration levels exceeded 90%. The colour change was complete once CO_2 levels reached 96%, indicating complete transition had occurred to **form-II**.
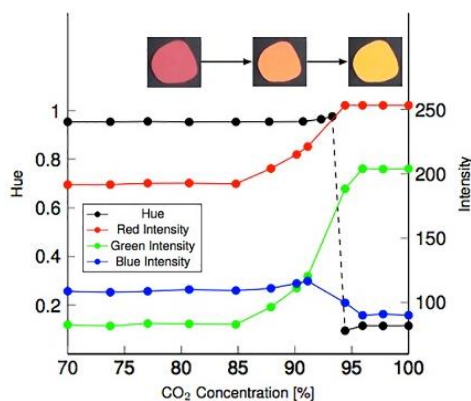
The colour change within the crystal is driven by desorption of water from the crystal structure. This effect causes a widening of the molecular arrangement and reduced overlap of d_{z^2} orbitals – see §3. The resultant effect is a blue-shift in the wavelength of light absorbed by the crystals, hence the perceived colour change from red to yellow. The shift in blue intensity is clearly shown in Fig. 10.

Fig. 11 shows the variation in hue and intensity values with CO_2 concentration in the through-flow for **form-II** to **form-I**. This experiment was conducted by initially purging the system with CO_2 and incrementally reducing the CO_2 concentration level from 100% in steps of 2-4%; in all cases the CO_2 level was monitored by infra-red gas analysis.

The crystal colour transition took place over a broader range of CO_2 levels, being triggered at ~65% and undergoing complete transition to **form-I** once CO_2 levels of 30% had been reached. The variation in intensity levels were also more gradual relative to the **form-I** to **form-II** experiments. In particular, green intensity levels were seen to exhibit the broadest activity over the widest range of CO_2 levels; green intensity levels changed from 204 to 84 over a 35% change in CO_2 concentration level.

As the *dry* CO_2 gas level was reduced, the *wet* ambient air constituted a larger component of the through-flow. The color change in the crystal was driven by the re-absorption of water from the increasingly humid through-flow, forming hydrogen bonds with available cyanide groups. The emergence of these bonds reduces the distance between molecular layers and hence increases the overlap of d_{z^2} orbitals. A red shift in the wavelength of light absorbed by the crystals occurs, indicated by a perceived color change from yellow to red.

Figure 11: Variation of intensity and hue with CO_2 concentration for transition from form-II to form-I (images of crystal shown inset)

Figures 10 and 11 show that the variation in hue is too sensitive for accurate sensing, whereas green intensity levels exhibited the most gradual transition from one form to the other; hence green intensity is used for all further calibrations.

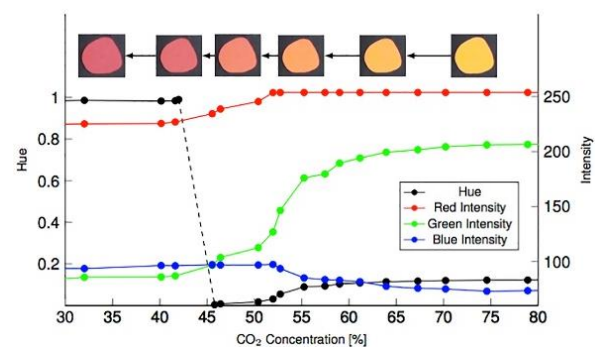The colour response (*i.e.* green intensity-CO_2 level relationship) is shown to be dependent on

Figure 10: Variation of intensity and hue with CO_2 concentration for transition from form-I to form-II (images of crystal shown inset)

whether the crystals are undergoing transition from **form-I** to **form-II** or **form-II** to **form-I**. This difference, termed a hysteresis, will be examined in greater depth in §5.2, along with the repeatability of the color change processes.

5.2 Hysteresis & repeatability

The repeatability of the vapochromic crystal behavior was assessed by repeating the experiments described in §5.1, focusing solely on the variation of green intensity with CO_2 concentration in the mainstream flow. The colour change processes were monitored in four separate tests, each beginning with the transition from **form-I** to **form-II** and subsequently **form-II** to **form-I** by firstly increasing the CO_2 injection and then reducing it, respectively. In all cases the CO_2 concentration level was monitored by the infra-red gas analyser.

Data from all four experiments are shown in Fig. 12. Both transitions follow a sigmoidal-shaped curve with significant hysteresis displayed. During the **form-I** to **form-II** transition the green intensity remains constant at a value of 84 until the CO_2 concentration is elevated above 85%. A gradual increase in green intensity is then seen up to a CO_2 concentration of 93%; a dramatic step-change in green intensity is seen between 93 and 95% CO_2, before which a constant value of 204 is reached.

The **form-II** to **form-I** transition occurred at a far lower concentration of CO_2. A noticeable reduction in green intensity was seen as the CO_2 level was reduced below ~65%; this controllable reduction in intensity continued until the CO_2 level fell to 30%.

These experiments demonstrate that the vapochromic crystals are non-hygroscopic, *i.e.* they lose water more readily than they adsorb it (with reference to Fig. 12, transition from **form-I** to **form-II** occurs more readily than from **form-II** to **form-I**). The reduced sensitivity of the crystal when adsorbing water naturally lends itself to a sensing application; the **form-II** to **form-I** transition will therefore be investigated from hereon in.
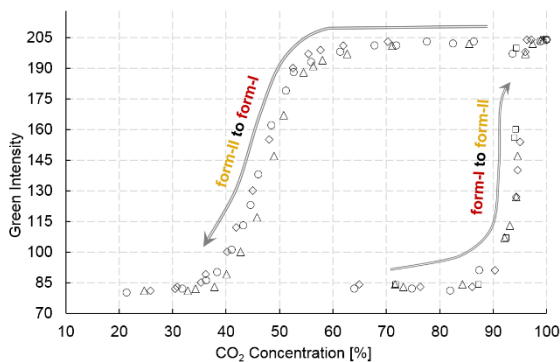
Figure 12: Variation of green intensity with CO_2 concentration for transition from i) form-I to form-II and ii) form-II to form-I. Symbols denote repeated tests.

The **form-II** to **form-I** transition includes a region of near-linear proportionality in the sigmoid-shaped curve - between CO_2 concentration levels of 55 and 40%. The sensitivity of this region indicated a change in green intensity of 6.9 per 1% change in CO_2 concentration level.

The repeatability of the **form-II** to **form-I** transition was assessed and is reproduced in Fig. 13, with error bars. The standard deviation from the mean of the measured values is shown for each test condition, highlighting a maximum error in green intensity of +/- 13.1. The error bars for the CO_2 concentration measured are based on §4.2. A treatment of the associated measurement error will be considered with respect to a practical application in §6.2.
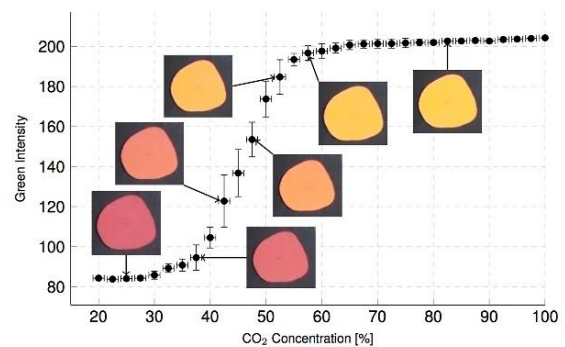

Figure 13: Repeatability of measurements of green intensity and CO_2 concentration for transition from form-II to form-I (images of crystal shown inset)

5.3 Effect of temperature

It has been previously shown (see Bryant [25, 26]) that the crystal transition between **form-II** to **form-I** is sensitive to temperature, *i.e.* an external heat source can be used to expedite the water desorption from the basic crystal.

The *elevated temperature* test plate was installed in the wind tunnel in order to provide an external heat source to the vapochromic crystal. The through-flow of air was initially maintained at 100% CO_2, *i.e.* the crystal was in **form-II**. The film-heater (see Fig. 7b) was used to raise the temperature of the copper block in which the glass slide and vapochromic crystal were housed. The temperature of the copper block was monitored throughout the test using a k-type thermocouple. Once at a constant temperature, the throughflow concentration was reduced from 100% CO_2 to ambient air in incremental steps (~2-3%); for all cases the CO_2 level was measured by infra-red gas analysis. The experiment was repeated at four different elevated temperatures, as shown in Fig. 14.
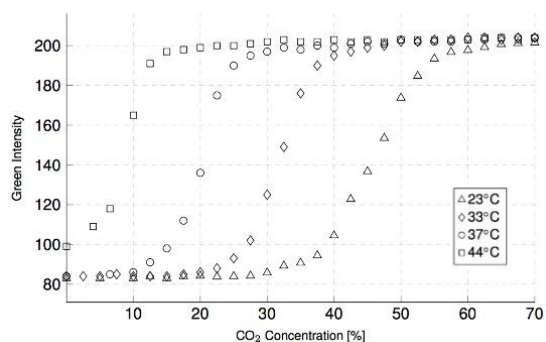
Figure 14: Effect of temperature on variation of green intensity with CO₂ concentration for transition from form-II to form-I

The effect of temperature on the chemical transition is significant. At 23 ºC the transition band occurred between CO_2 concentration levels of 65 and 30%; at 44 ºC the transition band occurred between 20 and 0% CO_2. Alternatively, the start of the transition band of the crystal was delayed by ~45% with a 21 ºC increase in crystal temperature. This important finding demonstrates the versatility of the vapochromic crystals, where temperature control could potentially be used to provide an experimental technique with a far wider range of sensing concentrations.

Moreover, the near-linear region of the form-II to form-I sigmoidal-shaped transition exhibits a change in gradient with temperature, *i.e.* changing the sensitivity of the crystal. The gradients of the near-linear regions are shown in Table 1.

Temperature (ºC)	Gradient
23	6.9
33	10.2
37	12.6
44	13.4

Table 1 Gradients of the near-linear region of the form-II to form-I sigmoid-shaped transition curve at elevated temperature

The external heating provides sufficient energy to break the hydrogen bonds between the water and cyanide groups within the vapochromic crystal. This process widens the distance between molecules, hence reducing overlap of d_{z^2} orbitals and causing a blue-shift in the absorbed wavelength of light. As discussed in §5.1, when the crystals are exposed to humid ambient air in form-II they adsorb water back into the structure and reform the hydrogen bonds. At elevated temperatures these bonds are harder to form and so the crystals require a higher concentration of humid air to aid transition to form-I. The transition band is clearly seen to approach lower CO_2 concentrations in Fig.14, in direct support of this theory.

At sufficiently high temperatures the crystals will fail to regain the required water content to transition

fully to form-I. This is demonstrated by the data at 44 ºC where the green intensity value remains at 100 despite the through-flow being fully ambient (*i.e.* without CO_2 injection).

5.4 Effects of viewing and illumination angle

Optical methods are often prone to sensitivities in viewing and illumination angles. An experiment was conducted to assess the impact of these angles on the measured values of green intensity and hue. The through-flow in the wind tunnel was controlled to create steady-state conditions at either ambient levels of CO_2 or 100% CO_2, *ergo* the crystals were either steady form-I or form-II, respectively. The illumination angle, θ, was varied from 0 to 45 degrees with the camera initially perpendicular to the test plate; the test was repeated with the camera moved *off-axis* at 45 degrees to the target plate. Images were captured for each of the defined test conditions and processed as described in §4.3. The imaging results are summarized in Table 2.

| Θ (deg) | θ (deg) | Green intensity | | Hue | |
		form-I	form-II	form-I	form-II
0	0	63	206	0.97	0.12
	30	83	204	0.97	0.12
	45	58	194	0.98	0.12
45	0	71	196	0.97	0.12
	30	90	161	0.97	0.10
	45	67	155	0.96	0.10

Table 2 Effect of viewing and illumination angles on processed images of the crystal in form-I and form-II.

Changes in green intensity levels are seen for variations in illumination angle and camera angle for both forms of the crystal; varying the illumination and viewing angles had minimal effect on the hue. This suggests that it was the perceived intensity of the captured image itself that was changing and not the colour of the crystal itself. A more detailed assessment of configuration angles would be required to assess the effect throughout the full colour-change process, however the data provided here support the case for a fixed illumination and viewing setup across comparable tests. This finding is consistent with that frequently observed for TLC measurements (*e.g.* Kakade *et al.* [8]).

5.5 Aging

To test the durability of the vapochromic transition, crystallites of the vapochromic complex were deposited on a glass slide through spin coating from dichloromethane solution. The slide was repeatedly passed through a dry nitrogen stream, inducing the form I to form II transition, at a rate of

0.6 Hz. After continuous cycling for a period of 6 hours (>10^4 cycles), no apparent change in the speed or colour intensity of the response was observed. Similarly, drop-cast films stored under ambient conditions retained their vapochromic behaviour for more than six months, again with no appreciable degradation in the response.

6 Application of vapochromic crystals to fluid dynamic experiments

Vapochromic crystals exhibit a reversible colour change based on the adsorption and desorption of water: as the water content of the crystals changes so too does the wavelength of light that they reflect (*i.e.* they change colour). Above a prescribed water content they are red – colour change from red to yellow occurs as the crystals lose water. Given that the water content of the crystals is directly related to humidity of the surrounding air, so too is the colour of the crystals. As such, the colour change of the crystals allows the humidity of the surrounding air to be measured.

Consider an experiment where two gas streams mix. If one stream is supplied as humid air and the other as a dry gas then the specific humidity of the resulting mixture will be different to that of the air at inlet. A layer of vapochromic crystals applied to a surface downstream of the mixing region could be used to directly measure the specify humidity of the gas at the surface. The specific humidity of the mixture can be related to the concentration level of the dry gas in the mixture through a simple mass balance (*i.e.* a dry gas can be used as a tracer when introduced to a humid air stream in the same way that a foreign gas can be when introduced to air). The humid air would need to be conditioned to a specific humidity, close to the prescribed humidity at which the crystals start to change colour. As such, in experiments where a humid gas mixes with a dry gas the change in colour of vapochromic crystals with humidity is analogous to a change in colour with trace gas concentration.

6.1 A practical example

To demonstrate the importance of concentration measurements to experimental fluid dynamists a practical example is provided. The example chosen is one involving the use of tracer gases and surface concentration measurements to investigate the mixing of fluid streams in gas turbine film cooling.

In modern gas turbine engines the main gas path temperature entering the turbine is often greater than the permissible working temperatures of the vane and blade materials. Coolant is ejected from numerous holes in the vanes and blades to provide a film that protects the surfaces from the high working temperatures in the region (Cumpsty and Heyes [29]). However, bleeding the coolant from the compressor is parasitic to the efficiency of the engine. Engine designers want a film cooling configuration that provides the necessary levels of cooling with minimal use of coolant. As such, a great deal of research has been undertaken in simplified experimental test facilities to quantify the performance of film-cooling configurations. Performance is generally assessed through measurement of adiabatic effectiveness (η), which is given by:

$$\eta = \frac{T_\infty - T_{ad}}{T_\infty - T_c} \qquad [1]$$

To determine the adiabatic effectiveness experimenters typically conduct heat transfer experiments with an adiabatic surface downstream of the film cooling geometry; measurement of the main gas path temperature (T_∞), the coolant temperature (T_c) and the steady-state surface temperature (T_{ad}) enable the adiabatic effectiveness to be determined. An alternative approach is to seed one of the flows (usually the coolant) with a trace gas. Concentration measurements are made downstream of the film cooling geometry on the surface. For a turbulent gas flow the concentration measurements collected under isothermal conditions with an impermeable wall are analogous to temperature measurements made in heat transfer experiments with an adiabatic wall. Under these conditions the thermal and concentration boundary layer profiles will be of the same functional form and so the heat and mass transfer analogy applies (Shadid and Eckert [30]). The adiabatic effectiveness can thus be determined in an isothermal experiment from:

$$\eta = \frac{c_\infty - c_{ad}}{c_\infty - c_c} \qquad [2]$$

where c_∞, c_c and c_{ad} are the measured mass fractions of trace gas for the mainstream, coolant and surface respectively.

Temperature based methods are prone to errors associated with the imperfect *quasi*-adiabatic boundary conditions; concentration based methods are a useful proxy where the boundaries are impermeable to gaseous exchange with the adjacent fluid. The vapochromic technique presented here has great potential for sensing local species concentration – *even when the impermeable surface is rotating,* as is the case frequently encountered in turbomachinery.

6.2 Measurement accuracy

An error analysis was conducted on the data shown in Figs. 12 and 13. A cubic spline interpolation was created for the calibration curve in Fig. 13; the 95% confidence interval is shown shaded in grey in Fig. 15.
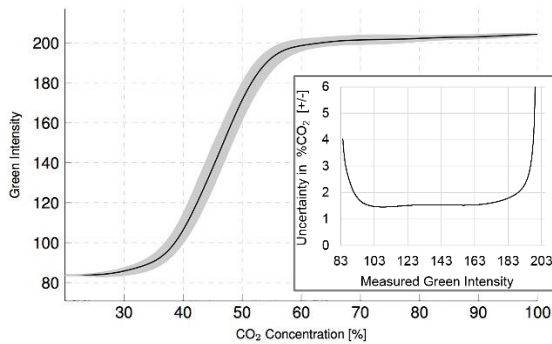
Figure 15: Variation of green intensity with CO_2 concentration for transition from form-II to form-I (line is a cubic spline fit to the data, shaded region represents the uncertainty interval)

The uncertainty in $\%CO_2$ is plotted against the measured green intensity, inset. The distribution of uncertainty shows an average value of $\pm1.5\%$ CO_2 over the range of green intensity values from 90-170. Outside this range of green intensity the error dramatically increases.

The authors expect that the error margin could be narrowed further should the experiments be conducted under more finely controlled ambient conditions (*i.e.* humidity and temperature). This would require that the mainstream flow be pre-conditioned prior to entry into the test section.

7   Conclusions

An extensive set of calibrations for vapochromic crystals has been presented, with the colour-change process being shown as green intensity-CO_2 concentration relationships. A purpose-built wind tunnel was designed to accommodate the crystals and instrumented for measurements of species concentration, pressure and temperature.

The colour-change process was shown to exhibit a pronounced hysteresis, whereby the adsorption (form-II to form-I) and desorption (form-I to form-II) of water into the crystal structures occured at independent CO_2 concentration bands. Increased sensitivity was seen in the form-II to form-I, making this process more suitable to a sensing process. Image processing revealed that green intensity demonstrated the greatest controllability (as opposed to hue); green intensity decreased by 6.9 per 1% change in CO_2 concentration level over the near-linear portion of the sigmoid-shaped calibration curve. The vapochromic crystals were assessed for repeatability and found to sense the local CO_2 concentration to $\pm1.5\%$ CO_2 over a range of green intensity values from 90 to 170.

A strong effect of surface temperature was shown, delaying the transition band of the crystals by ~45% with a 21 °C increase in crystal temperature. Temperature was also shown to have a marked effect on the gradient of the near-linear portion of the calibration curves.

As is typical with optical methods, the viewing and illumination angles were shown to affect the crystal calibrations. Should vapochromic crystals be applied to fluid dynamic experiments then the calibration should be undertaken *in-situ*. It is hoped that the work presented in this paper demonstrates the suitability of vapochromic crystals for experimental research.

References

[1] Sangan, C. M., Pountney, O., Zhou, K., Wilson, M., Owen, J. M. and Lock, G., 2013. "Experimental measurements of ingestion through turbine rim seals. Part 1: Externally induced ingress". Journal of Turbomachinery: Transactions of the ASME, 135(2), 021012.

[2] Han, J.C. & Rallabandi, A.P., 2010. "Turbine Blade Film Cooling Using PSP Technique." Frontiers in Heat and Mass Transfer, 1(1), 013001.

[3] Kasagi, N., Moffat, R. J. and Hirata, M., 1989, Liquid crystals, In: Handbook of Flow Visualization (Ed. Yang, W.J). New York: Hemisphere, pp. 105-124.

[4] Ireland, P. T. and Jones, T. V., 2000, "Liquid crystal measurements of heat transfer and surface shear stress," Meas. Sci. Technol., 11(7), pp. 969-986.

[5] Pountney, O.J., Sangan, C.M., Lock, G. D. and Owen, J. M., 2013. "Effect of ingestion on temperature of turbine discs," Journal of Turbomachinery: Transactions of the ASME, 135(5), 051010.

[6] Baughn, J. W., 1995, "Liquid-crystal methods for studying turbulent heat transfer," Int. J. Heat Fluid Flow, 16(5), pp. 365-375.

[7] Abdullah, N., Abu Talib, A. R., Saiah, H. R. M., Jaafar, A. A. and Salleh, M. A. M., 2009, "Film thickness effects on calibrations of a narrowband thermochromic liquid crystal," Exp. Therm. Fluid Sci., 33(4), pp. 561-578.

[8] Kakade, V. U., Lock, G. D., Wilson, M., Owen, J. M. and Mayhew, J. E., 2009, "Accurate heat transfer measurements using thermochromic liquid crystal. Part 1: Calibration and characteristics of crystals," Int. J. Heat Fluid Flow, 30(5), pp. 939-949.

[9] Anderson, M. R. and Baughn, J. W., 2004, "Hysteresis in liquid crystal thermography," ASME J. Heat Transfer, 126(3), pp. 339-346.

[10] Anderson, M. R. and Baughn, J. W., 2005, "Liquid-crystal thermography: Illumination spectral effects. Part 1 - experiments," ASME J. Heat Transfer, 127(6), pp. 581-587.

[11] Camci, C., Kim, K., Hippensteele, S. A. and Poinsatte, P. E., 1993, "Evaluation of a hue capturing based transient liquid-crystal method for high-resolution mapping of convective heat-transfer on curved surfaces," ASME J. Heat Transfer, 115(2), pp. 311-318.

[12] Farina, D. J., Hacker, J. M., Moffat, R. J. and Eaton, J. K., 1994, "Illuminant invariant calibration of thermochromic liquid crystals," Exp. Therm. Fluid. Sci., 9(1), pp. 1-12.

[13] McKeon, B.J. and Engler, R.H., 2007, Pressure Measurement Systems. In: Tropea, C., Yarin, A.L. and Foss, J.F. (eds.) Experimental Fluid Mechanics. Berlin Heidelberg: Springer-Verlag, pp.179-214.

[14] Liu, T. and Sullivan, J.P., 2005. Pressure and Temperature Sensitive Paints. 1st ed., Berlin Heidelberg: Springer-Verlag.

[15] Klewicki, J.C., Saric, W.S., Marusic, I. and Eaton, J.K., 2007, Wall-Bounded Flows. In: Tropea, C., Yarin, A.L. and Foss, J.F. (eds.) Experimental Fluid Mechanics. Berlin Heidelberg: Springer-Verlag, pp.871-907.

[16] Tanner, L.H. and Blows, L.G., 1976, "A study of the motion of oil films on surfaces in air flow with application to the measurement of skin friction," J. Physics E: Scientific Instruments, 9, 3

[17] Naughton, J.W. and Sheplak, M., 2002, Modern developments in shear stress measurement. Prog. Aerosp. Sci, 32, pp. 515-570.

[18] Kato, M., 2007, Luminescent platinum complexes having sensing functionalities. Bull. Chem. Soc. Jpn., 80, 287-294.

[19] Grove, L. J., Rennekamp, J. M., Jude, H. & Connick, W. B., 2004, A new class of platinum(II) vapochromic salts, J. Am. Chem. Soc., 126, 1594-1595.

[20] Grove, L. J., Oliver, A. G., J. A. Krause & Connick, W. B., 2008, Structure of a crystalline vapochromic platinum(II) salt, Inorg. Chem., 47, 1408-1410.

[21] Shigeta, Y. et al., 2016, Shape-memory platinum(II) complexes: intelligent vapor-history sensor with ON-OFF switching function, Chem. Eur. J., 22, 2682-2690.

[22] Kunugi, Y., Mann, K. R., Miller, L. L. & Exstrom, C. L., (1998), A vapochromic LED, J. Am. Chem. Soc., 120, 589-590.

[23] Kobayashi, A., Yonemura, T., & Kato, M., 2010, Vapour-induced amorphous-crystalline transformation of a luminescent platinum(ii)-diimine complex, Eur. J. Inorg. Chem., 2465-2470.

[24] Aliprandi, A. Matteo, M. & De Cola, L, 2016, Controlling and imaging biomimetic self-assembly, Nat. Chem., 8, 10-15.

[25] Bryant, M. J., Skelton, J. M. et. al., 2017, A rapidly-reversible absorptive and emissive vapochromic Pt(II) pincer-based chemical sensor, Nature Comm., 8, 1-9.

[26] Bryant, M.J., 2015, "Platinum pincer complexes: In pursuit of switchable materials," PhD Thesis, University of Bath.

[27] Cho, G.H., Tang, H., Owen, J.M. & Lock, G.D., 2016, "On the measurement and analysis of data from transient heat transfer experiments," Int. J. Heat & Mass Trans., 96, pp. 268-276.

[28] Baughn, J.W., Anderson, M.R., Mayhew, J.E. & Wolf, J.D., 1999, "Hysteresis of thermochromic liquid crystal temperature measurement based on hue," ASME J. Heat Transf., 121, 1067-1072.

[29] Cumpsty, N. and Heyes, A., 2015, Jet propulsion. 3rd ed., Cambridge: Cambridge University Press.

[30] Shadid, J.N. and Eckert, E.R.G., 1991. The Mass Transfer Analogy to Heat Transfer in Fluids with Temperature-Dependent Properties. Journal of Turbomachinery: Transactions of the ASME, 113(1), pp. 27-33.